Functional Connectivity from EEG Signals during Perceiving Pleasant and Unpleasant Odors

Abstract—**The olfactory sense is strongly related with memory and emotional processes. Studies on the effects of odor perception from brain activity have been conducted by using different neuro-imaging techniques. In this paper, we analyse electroencephalography (EEG) of 23 subjects during perceiving pleasant and unpleasant odor stimuli. We describe the construction of brain functional connectivity networks measured by most commonly used models. We discuss the network-based features of functional connectivity, as well as design classifiers by applying different functional connectivity network features. Finally, we show that the brain can be seen as a nonlinear small-world network, and by extracting appropriate features we manage to classify pleasant and unpleasant olfactory perceptions with a significantly non-random average Kappa value of 0.11 ± 0.16.**

Index Terms—**functional connectivity, odor pleasantness, EEG, nonlinear regression analysis, Granger causality**

I. INTRODUCTION

Multimedia systems are increasingly becoming immersive, in order to evoke strong emotions and render user-experience more realistic. Traditionally, multimedia systems include video and audio contents, they, thus, mainly stimulate the visual and auditory senses. Nevertheless, recently odors have started to be incorporated into multimedia systems (e.g., [1]–[3]), since they directly stimulate memories and elicit strong emotions. However, emotion elicitation from odors has not been adequately investigated, although the primary response to smell is related to pleasantness perception [4].

Perception of pleasantness from various stimuli has been investigated by various researchers through different means. Many studies have been conducted on the investigation of pleasantness perception through facial expressions [5], food intake [6], languages [7], etc. Research on pleasantness detection and classification has been carried out by analyzing brain activity using various brain imaging techniques (e.g., [8]–[10]).

Although pleasantness perception has been thoroughly analysed for various, especially audiovisual, stimuli, it has received less attention during experience of odors. Moreover, various electroencephalography (EEG) studies on investigating odor pleasantness have analysed brain activation in terms of power spectral density features (e.g., [10]–[12]), but further information from EEG could contribute to a better understanding of pleasantness perception from odors. For instance, a question that still remains unanswered is regarding the way in which odor pleasantness influences functional connectivity patterns in remote brain locations. The hypothesis is that there are differences in the functional connectivity patterns when subjects experience pleasant and when they experience unpleasant

odors. However, it is still unclear what type of network the brain can be seen as during olfactory perception, and if there are network-based features able to discriminate pleasant and unpleasant odors.

The concept of functional connectivity maps has been largely used in neuro-imaging analysis to study various disorders with respect to control states, such as for instance major depression [13] and epilepsy [14]. Based on the neurophysiological principle [15], brain can be viewed as a complex network. Thus in this paper, we introduce the concept of functional connectivity to investigate the networking of the brain during odor pleasantness perception.

Since the dependence between different sub-regions of the brain can be interpreted in different ways, there exist different models of estimating functional connectivity in the brain. Widely used models include *Granger Causality* [16], *Transfer Entropy* [17], *Nonlinear Regression Analysis* [18] and *Spectral Coherence* [19]. In this paper, we apply and compare Granger causality and nonlinear regression analysis. In order to quantify differences in the estimated networks, we extract network-based features such as *characteristic path* [20], *local and global efficiency*, *clustering coefficient* [21], *shannon entropy* and *von Neumann entropy* [22]. The extracted features are then used for classification of perceived odor pleasantness.

The rest of the paper is organised as follows: Section II describes the experimental protocols and methods for constructing and measuring functional connectivity maps from EEG signals. Section III provides the classification results on pleasantness by using network-based features extracted from the functional connectivity maps. Section IV gives the conclusions of this work.

II. BACKGROUND

Multimedia systems are increasingly becoming immersive, in order to evoke strong emotions and render user-experience more realistic. Traditionally, multimedia systems include video and audio contents, they, thus, mainly stimulate the visual and auditory senses. Nevertheless, recently odors have started to be incorporated into multimedia systems (e.g., [1]–[3]), since they directly stimulate memories and elicit strong emotions. However, emotion elicitation from odors has not been adequately investigated, although the primary response to smell is related to pleasantness perception [4].

Perception of pleasantness from various stimuli has been investigated by various researchers through different means. Many studies have been conducted on the investigation of pleasantness perception through facial expressions [5], food

intake [6], languages [7], etc. Research on pleasantness detection and classification has been carried out by analyzing brain activity using various brain imaging techniques (e.g., [8]–[10]).

Although pleasantness perception has been thoroughly analysed for various, especially audiovisual, stimuli, it has received less attention during experience of odors. Moreover, various electroencephalography (EEG) studies on investigating odor pleasantness have analysed brain activation in terms of power spectral density features (e.g., [10]–[12]), but further information from EEG could contribute to a better understanding of pleasantness perception from odors. For instance, a question that still remains unanswered is regarding the way in which odor pleasantness influences functional connectivity patterns in remote brain locations. The hypothesis is that there are differences in the functional connectivity patterns when subjects experience pleasant and when they experience unpleasant odors. However, it is still unclear what type of network the brain can be seen as during olfactory perception, and if there are network-based features able to discriminate pleasant and unpleasant odors.

The concept of functional connectivity maps has been largely used in neuro-imaging analysis to study various disorders with respect to control states, such as for instance major depression [13] and epilepsy [14]. Based on the neurophysiological principle [15], brain can be viewed as a complex network. Thus in this paper, we introduce the concept of functional connectivity to investigate the networking of the brain during odor pleasantness perception.

Since the dependence between different sub-regions of the brain can be interpreted in different ways, there exist different models of estimating functional connectivity in the brain. Widely used models include *Granger Causality* [16], *Transfer Entropy* [17], *Nonlinear Regression Analysis* [18] and *Spectral Coherence* [19]. In this paper, we apply and compare Granger causality and nonlinear regression analysis. In order to quantify differences in the estimated networks, we extract network-based features such as *characteristic path* [20], *local and global efficiency*, *clustering coefficient* [21], *shannon entropy* and *von Neumann entropy* [22]. The extracted features are then used for classification of perceived odor pleasantness.

The rest of the paper is organised as follows: Section II describes the experimental protocols and methods for constructing and measuring functional connectivity maps from EEG signals. Section III provides the classification results on pleasantness by using network-based features extracted from the functional connectivity maps. Section IV gives the conclusions of this work.

III. MATERIALS AND METHODS

A. Experiments

A total of 23 right-handed subjects took part in the experiment (9 females, 14 males, 24 ± 4.6 years old). All subjects were non-smokers and without respiration problems. According to their self-reports, none had a history of injury in the olfactory bulb or incapability of smelling. Subjects were informed about the experimental protocol and the purpose of the study. None of the participants in experiment were wearing perfumed products on the day of experiment.

10 different odors were provided for the experiment, including rose water, lavender oil, jasmine oil, chocolate powder, mint oil, valerian pills, garlic powder, star anise, rotten cooked cauliflower and baby shampoo. The odorants were placed inside covered bottles so as to avoid effects of their visual characteristics.

After the set up of the EEG recording system, subjects were asked to relax and close their eyes. One odor bottle was randomly selected and provided to the subject's nostrils at 1-2 cm. The subjects were not informed about the name of the odor during the experiment. The same odor was presented for about 15 times, leading to about 15 trials. Each trial consisted of 6 seconds baseline and 6 seconds odor experience. After experiencing an odor, the subjects were asked to rate it in terms of pleasantness, using a 5-point Linkert scale that ranged from very unpleasant to very pleasant.

Regarding the equipment, an EGI's Geodesic EEG system (GES) 300 was used to record, amplify and digitalize the EEG signals. EEG signals were recorded from a 256-channel EEG Net Amps 300 cap with sampling frequency of 250Hz.

B. Pre-processing of EEG Signals

Signals from 40 electrodes which are placed on face muscles and around eyes are manually rejected for all subjects due to movement artifacts. Signals from the remaining 216 electrodes are kept for further analysis.

A bandpass filter (4th order butterworth) is applied for the EEG signals with pass-band 3-47 Hz. A small laplacian filter is applied for each electrode in order to reduce volume conduction effects [23]. Further artifacts are rejected by using Independent Component Analysis (functions are provided by EEGLAB© toolbox [24]).

C. Construction of Brain Networks

Brain connectivity refers to a patter of anatomical links (anatomical connectivity) or of statistical dependencies (functional connectivity) between neural assemblies. The functional connectivity pattern is represented by statistical or causal relationships estimated using measures such as cross-correlation, coherence or information flow [25]. Brain connectivity is a crucial concept to elucidate how neural networks process information. In this paper, we investigate functional connectivity and use this information to interpret how brain functions during perception of pleasant and unpleasant odors.

Functional connectivity can be estimated in various ways. For instance, a neurophysiological concept of functional connectivity is introduced by Wendling's group, who used the Nonlinear Regression Analysis as a measure of functional connectivity [26]. The notion of Granger Causality [27] has been also extensively used to estimate functional connectivity.

1) Granger Causality: Granger causality is first proposed by C.W.J. Granger in investigating causal relations in econometric models in 1969 [16]. Decades later this concept is

introduced into various neurophysiological studies. It is used to measure the causality between activities in different neuron assemblies, which estimates the functional connectivity over brain regions.

Suppose we have two time series X_t and Y_t. Let U_t denote all the information accumulated from both time series since time $t-1$, and $U_t - Y_t$ denotes all this information apart from the specified series Y_t. $\sigma^2(X|U)$ is the variance of $\epsilon_t(X|U)$, in which $\epsilon_t(X|U) = X_t - P_t(X|U)$ and $P_t(X|U)$ represents the optimal, unbiased, least-squares predictor of X using the set of values U.

Definition of Causality: If $\sigma^2(X|U) < \sigma^2(X|\overline{U-Y})$, then Y is causing X, denoted by $Y_t \Rightarrow X_t$. Under the notion of Granger causality, Y_t is causing X_t if X_t is better predicted using all available information than if the information from Y_t is excluded.

The definition of Granger causality represents a theoretic approach which is difficult to implement due to lack of knowledge of the distributions of the estimators. In order to solve this problem, different approaches for computing Granger causality have been developed. In this paper we use the Vector Auto-Regression model (VAR) [28] to estimate Granger causality since it provides better computational efficiency and numerical accuracy [28].

According to the VAR model, we suppose signals from two channels (i.e., two electrodes in our case) are $\mathbf{X_t}$ and $\mathbf{Y_t}$. Then

$$\mathbf{U_t} = \begin{pmatrix} \mathbf{X_t} \\ \mathbf{Y_t} \end{pmatrix} = \sum_{k=1}^{p} \begin{pmatrix} A_{xx,k} & A_{xy,k} \\ A_{yx,k} & A_{yy,k} \end{pmatrix} \begin{pmatrix} \mathbf{X_{t-k}} \\ \mathbf{Y_{t-k}} \end{pmatrix} + \begin{pmatrix} \epsilon_{\mathbf{x,t}} \\ \epsilon_{\mathbf{y,t}} \end{pmatrix} \tag{1}$$

U_t represents the combined time series by X_t and Y_t, which will be used in VAR model for regression and analysis of dependence between X_t and Y_t. The residuals covariance matrix Σ from the residual terms in (1) is estimated as

$$\Sigma \equiv cov \begin{pmatrix} \epsilon_{\mathbf{x,t}} \\ \epsilon_{\mathbf{y,t}} \end{pmatrix} = \begin{pmatrix} \Sigma_{xx} & \Sigma_{xy} \\ \Sigma_{yx} & \Sigma_{yy} \end{pmatrix}. \tag{2}$$

In this paper we use the MVGC toolbox [28] to estimate the parameters in the VAR model. We first estimate the best model order p by using the AIC (Akaike Information Criterion). The minimum model order is selected by using a regression model of Morf's version of the LWR (the initials stand for Levinson, Whittle, Wiggins and Robinson) algorithm [29]. Similarly to the estimation of the model order, the LWR is also used for estimating the VAR parameters. The Granger causality from $\mathbf{Y_t}$ to $\mathbf{X_t}$ is then defined as:

$$F_{\mathbf{Y_t} \rightarrow \mathbf{X_t}} \equiv ln \frac{|\Sigma'_{xx}|}{|\Sigma_{xx}|}. \tag{3}$$

In Equation (3), $|\Sigma'_{xx}|$ represents the covariance matrix of the reduced regression (the regression contains only $\mathbf{X_t}$, and $\mathbf{X_t}$ is predicted only by information from its own past), while $|\Sigma_{xx}|$ represents the covariance matrix of the full regression (which contains both $\mathbf{Y_t}$ and $\mathbf{X_t}$). Thus, the value of F provides the "amount of information" transmitted from $\mathbf{Y_t}$ to $\mathbf{X_t}$ by
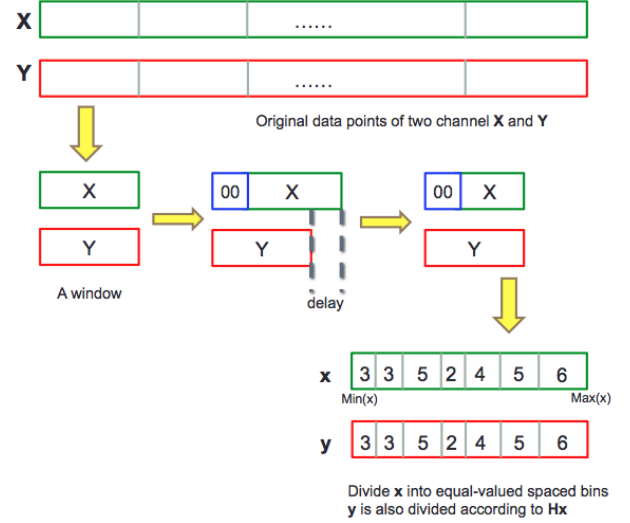

Fig. 1. An example of separating EEG time series into windows and bins for computing the nonlinear regression curves

estimating the reduction in the prediction error when $\mathbf{Y_t}$ is included in the prediction of $\mathbf{X_t}$. When there is no information transmitted from $\mathbf{Y_t}$ to $\mathbf{X_t}$ (i.e., $|\Sigma'_{xx}| = |\Sigma_{xx}|$), then $F = 0$. There is no upper limit on the values of F.

2) Nonlinear Regression Analysis: Nonlinear regression analysis is also a commonly used way to estimate the functional connectivity, which is represented by statistical coupling between EEG signals. This method is introduced by Pijin and Lopes Da Silva for EEG analysis [18]. Nonlinear regression analysis can quantify the relationships between different EEG signals in order to determine whether activity in one neuron assembly depends on that of other assemblies. Suppose we have two channels of EEG signals x and y, then nonlinear regression analysis provides a measure called *correlation ratio* η^2, whose estimator is called h^2. η^2 (or h^2) gives a statistical measure that describes the dependency of signal x on y. Assume the amplitude of signal y is a function of the amplitude of signal x. The expectation of y given a value of x is denoted as $\mu_{y|x}$ where:

$$\mu_{y|x} = \int_{-\infty}^{\infty} yp(y|x)\mathrm{d}y, \tag{4}$$

and $\mu_{y|x}$ describes the predicted value of y given x. By this definition, we can calculate η^2, which represents the reduction of variance of y that obtained by predicting y value using $\mu_{y|x}$. η^2 is expressed as:

$$\eta^2 = \frac{Total\ Variance - Unexplained\ Variance}{Total\ Variance} \tag{5}$$

Explained variance is the variance calculated from y according to $\mu_{y|x}$. In this paper, the nonlinear regression analysis algorithm is implemented by fieldtrip toolbox© [30]. the procedure is depicted in Fig. 1).
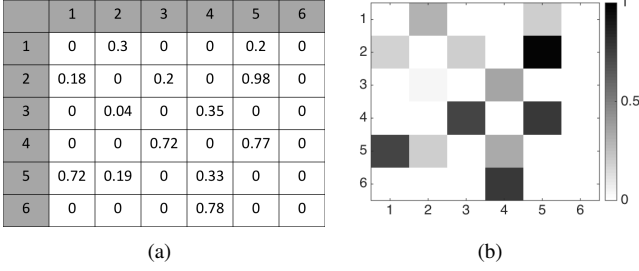
	1	2	3	4	5	6
1	0	0.3	0	0	0.2	0
2	0.18	0	0.2	0	0.98	0
3	0	0.04	0	0.35	0	0
4	0	0	0.72	0	0.77	0
5	0.72	0.19	0	0.33	0	0
6	0	0	0	0.78	0	0

(a)   (b)

Fig. 2. An example of a weighted functional connectivity map of size 6×6. In (a) the values represent the weights of the nodes. Each weight corresponds to the value of the underlying functional connectivity map. (b) A visual presentation of the same weighted functional connectivity map.

D. Significance Check

The significance check is similar for both methods (Grancer causality and Nonlinear Regression Analysis) and is split into two main parts: (1) p-value calculation for samples based on theoretical asymptotic null distribution; (2) statistical significance adjusted for *Bonferroni* correction. The rationale behind applying a significance check is to keep only the significant connections.

The *null hypothesis* H_0 is set to "there is no functional connectivity between two channels". In this paper, we assume that the connectivity values emanate from a normal distribution and the p-value that rejects the null hypothesis is set to $p = 0.05$. The commonly used F-statistics is applied for estimating the p-value both for Granger Causality and for Nonlinear Regression Analysis.

All the values in functional connectivity maps that passed significance check are kept for feature extraction and classification in later steps. In order to keep the information about the strength of the connections, we use weighted maps. The weights emanate from the original values of the functional connectivity maps (estimated either with Granger causality or with nonlinear regression analysis) that survived the significance check (an example is presented in Fig. 2).

E. Network Feature Extraction

The functional connectivity maps give us a view of how channels communicate information with each other, thus we can consider this map as a network. Different ways of treating brain networks have been proposed by different groups. For instance, some research groups see the brain as a scale-free network [31], while others view it as a small-world network [32]. In this section, we introduce two categories of network features, based on the principles of scale-free networks and of small-world networks, namely – *physical statistics* features for scale-free networks, and *graph theory-based* features for small-world networks.

1) Small-World Network Features: A small-world network consists of nodes that can be reached from every other node with a small number of steps. Different aspects of small-world networks have been studied and here, based on the commonly used features in neural network studies, we introduce four

features for analysing the functional connectivity maps which are *characteristic path*, *global efficiency*, *local efficiency* and *clustering coefficient* [20] [21].

Characteristic path represents the average shortest path of the network. The minimum value is achieved when the network is a complete graph (every pair of distinct vertices is connected by a unique edge). In our case, we can interpret the characteristic path as a feature representing the number of connections in the functional connectivity networks. The more the connections in the functional connectivity network, the smaller the value of the characteristic path, thus the faster the information that is transferred through the network.

The concept of *global efficiency* of a small-world network is introduced by Latora and Marchiori [21] and provides a measure of efficient behaviour of the network, by assuming that the network system is parallel (i.e., every vertex sends information concurrently through its edges in the network). The global efficiency of the network is higher when the characteristic path is short. Thus, global efficiency measures how efficiently the vertices exchange information through the network concurrently. Similarly with global efficiency, *local efficiency* is defined as the average efficiency of the subgraphs of the neighbours of a vertex i in the graph (details of computing subgraphs can be referred to [33]). The subgraphs of i do not contain vertex i, hence, the local efficiency can show how efficient the communication is when i is removed from the network. Thus the local efficiency reveals how much the network is fault tolerant.

Finally, *clustering coefficient* of a network measures the degree to which vertices in a graph tend to cluster together. The overall level of clustering in a network is given by Watts and Strogatz [20] as the average of the local clustering coefficients of all vertices.

2) Scale-Free Network Features: Although graph theory has been successfully used to describe brain functional connectivity networks, a few studies have shown that brain functional connectivity can also be considered as a scale-free network. An example of a scale-free compared to a random network is presented in Fig. 3. The number of links k of a node in a scale-free network follows a power law distribution as (6).

$$P(a\ node\ having\ k\ links) \sim k^{-\lambda} \qquad (6)$$

where λ is a parameter valued in the range $2 < \lambda < 3$. Groups of CJ Stam [34] have found that brain functional connectivity network can be viewed as a scale-free network because the connectivity distribution followed a power-law scaling with an exponent close to two.

In information theory, *entropy* plays an important role in measuring uncertainty. Recently, following theoretical and statistical mechanics paradigms, several entropy measures for complexity have been proposed for network structures, and these measures have shown good performance in quantifying the level of organisation encoded in structural features of scale-free networks. It is well known that *Shannon entropy* and *von Neumann entropy* are related to the information present in classical and quantum systems respectively. Both of them
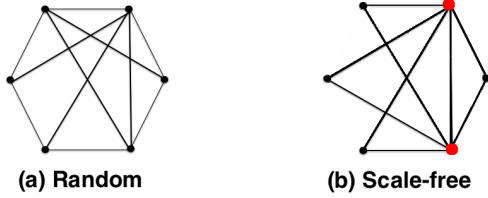
Fig. 3. An example of a random network (a) compared with a scale-free network (b) . Red nodes in (b) represent the hubs holding connections in the subgraph.

can be used to analyse the structural organisation of scale-free networks [35].

The amount of *Shannon entropy* has a correlation with the number of network structural constraints. Examples of network constrains include: a) fixed number of links per vertex, b) given degree sequence (a monotonic non-increasing sequence of the degrees of vertices in the graph), and c) community structure (vertices of the network can be easily grouped into sets of vertices such that each set of vertices is densely connected internally). From this point of view, we can conclude that Shannon entropy has a clear interpretation of quantifying the information presented in network structure (Detailed proof can be referred to [35]). If a network has a smaller Shannon entropy, it will have more constrains on its structure, which shows this network is more optimal.

Von Neumann entropy has been defined by von Neumann for proving the irreversibility of quantum measurement processes. Recently it is also shown that von Neumann entropy can also be applied to network analysis [22]. It has been shown that von Neumann entropy is a measure of regularity of networks [22]. For a fixed number of edges, regular networks (networks whose vertices have the same number of neighbours) have in general a higher von Neumann entropy. It is also shown that von Neumann entropy depends on the number of connected components, long paths and nontrivial symmetries. With a fixed number of edges, von Neumann entropy is smaller for networks with higher degree of cluster. The mathematical proofs can be found in [22] and [35].

Thus, to sum up, network-based features including characteristic path, local efficiency, global efficiency, clustering coefficient, Shannon entropy and von Neumann entropy are extracted from the estimated functional connectivity maps for classification purposes.

F. Classification

Support vector machine with a *Gaussian radial basis function* kernel is used for classification. The parameter selection of σ in RBF kernel is based on cross-validation. In particular, the dataset is split into three parts, namely training, validation and testing. Leave-one-subject-out (LOO) cross-validation is carried out to estimate the parameter σ. The testing is also carried out in a LOO cross-validation scheme. We tested 13 different values of parameter σ ranged from 0.01 to 2. More

specifically, the parameter σ is selected based on the training and validation using data from 22 subjects, while one subject is left out for testing. The procedure is repeated until all subjects have been left out as test-subjects (i.e., the procedure is repeated 23 times).

Cohen's Kappa κ [36], is a measure of agreement between two viewers, and is calculated to evaluate the classifier's performance. In our case the two viewers actually correspond to the ground truth and test labels. Cohen's kappa is considered an accurate metric for classification performance and takes into account unbalanced classes (i.e., classes with different number of samples).

IV. RESULTS AND DISCUSSION

The classification results for the features extracted from the functional connectivity maps are shown in Fig. 4. Higher kappa values indicate better classification performance. A kappa value $k = 0$ indicates a random decision. According to Figure 4, a higher classification performance is achieved with Nonlinear Regression Analysis compared to Granger's causality. In order to investigate if the kappa values are significantly non-random, a one-way *Student-t test* is applied for each case. The null hypothesis is that the kappa values for each case follow a Student distribution with zero mean. The null hypothesis is rejected for the case of Nonlinear Regression Analysis ($p < 0.05$, κ values with $\mu = 0.06, \sigma = 0.14$). Although this value is statistically significant, it is still close to zero. However, 14 out of 23 subjects have kappa values larger than zero. The null hypothesis is not rejected for the Granger causality case. The most representative kappa descriptives are summarised in Table I. The findings indicate that nonlinear patterns occur in the functional connectivity of neural assemblies, able to discriminate between pleasant and unpleasant odors.

TABLE I
KAPPA DESCRIPTIVES FOR EACH CLASSIFICATION SCENARIO. MIN STANDS FOR MINIMUM KAPPA VALUE, MAX FOR MAXIMUM KAPPA VALUE, AND SD FOR STANDARD DEVIATION. ONE ASTERISK INDICATES SIGNIFICANCE WITH $p < 0.05$, AND TWO ASTERISKS WITH $p < 0.01$.

Features	Min	Max	Mean	SD
GC	-0.2	0.77	0.07	0.23
NRA*	-0.2	0.19	0.06	0.14
GC+NRA*	-0.07	0.05	0.42	0.08
Characteristic path**	-0.1	0.45	0.096	0.15
Local efficiency**	-0.14	0.37	0.09	0.14
Global efficiency**	-0.17	0.5	0.11	0.17
Clustering coefficient**	-0.15	0.5	0.11	0.16
Shannon entropy	-0.13	0.34	0.07	0.12
von Neumann entropy	-0.13	0.3	0.01	0.12

In order to further investigate the classification performance of the two feature-categories, namely the small-world network and the free-scale network features, a SVM classifier is trained and tested as previously, for each individual feature.

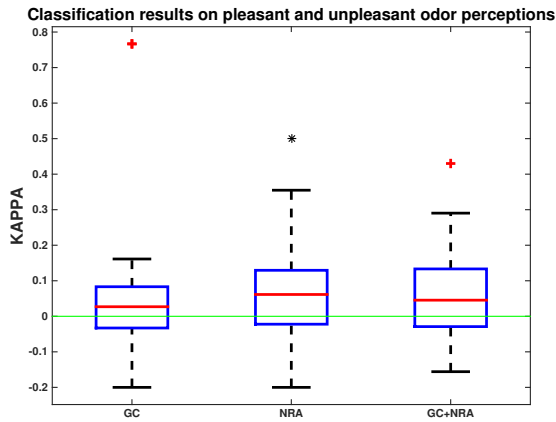**Classification results on pleasant and unpleasant odor perceptions**

Fig. 4. Cohen's Kappa results boxplots. On each box, the central (red) line represents the median value, the upside and downside edges represent the 25th and 75th percentiles, and the red crosses represent outliers. The green line represents the random decision, $Kappa = 0$. GC refers to the kappa values estimated for features extracted from the functional connectivity maps estimated using Granger Causality. NRA refers to the kappa values estimated for features extracted from the maps estimated using Nonlinear Regression Analysis. GC+NRA refers to the kappa values estimated using features both from Granger Causality and from Nonlinear Regression Analysis.

A one-way *Student-t test* is applied as previously to test the significance of the results. The results are presented in Table I. The results reveal that the small-world network features lead to a significantly non-random performance ($p < 0.01$), whereas this is not the case for the free-scale network features ($p > 0.05$). This result indicates that odor pleasantness perception can be depicted in small-world network features extracted from the functional connectivity across neural assemblies which is estimated using Nonlinear Regression Analysis.

The above findings reveal that functional connectivity maps estimated from EEG signals during olfactory perception can be mainly seen as non-linear small-world networks. Small-world networks are typically between regular and random in their structure, and resemble the structure of social networks. According to additional properties of small-world networks, they have high modularity, i.e., they consist of groups of nodes that cluster together in a more dense way than with the rest of the nodes. These characteristics of the small-world networks can be quantified using appropriate features, to distinguish perceived odor pleasantness. However, the obtained accuracy, although significantly non-random, is not very high. We expect that integrating information from the brain functional connectivity with commonly used features for odor pleasantness perception (such as for instance power spectral density features) can increase the classification performance.

Additionally, free-scale networks are known for their property of self-similarity in finer scales. However, in our case free-scale network features did not lead to significantly non-random results, indicating that self-similar properties of functional connectivity maps may not be responsible for odor pleasantness discrimination. These findings in general can have a great impact in affective computing, because they can obtain additional information about underlying emotional processes. Due to the limitations of research on odors (still many questions open regarding exposition time, etc.), it would be very interesting to further explore if similar patterns occur and if the classification performance is increased using more conventional affective stimuli, such as video and audio.

V. CONCLUSION

The concept of functional connectivity maps has been used to study the brain activity but it has not yet been used for classifying odor pleasantness perception. In this paper, we compared different methods of estimating functional connectivity from EEG signals for 23 subjects in order to classify pleasant and unpleasant odors. By considering the connectivity maps as networks, physical statistics and graph theory based features were extracted and used in SVM classifiers. The best classification accuracy based on Cohen's Kappa was achieved using nonlinear regression analysis and small-world network features to estimate the connectivity maps. The results indicated that nonlinear patterns occur in the connectivity maps during hedonic olfactory perception, able to classify odor pleasantness perception in a significantly non-random way.

REFERENCES

[1] T. Nakamoto, H. Ishida, and H. Matsukura, "Olfactory display using solenoid valves and fluid dynamics simulation," *Multiple Sensorial Media Advances and Applications: New Developments in MulSeMedia*, p. 140, 2011.

[2] T. Nakamoto, S. Otaguro, M. Kinoshita, M. Nagahama, K. Ohinishi, and T. Ishida, "Cooking up an interactive olfactory game display," *Computer Graphics and Applications, IEEE*, vol. 28, no. 1, pp. 75–78, 2008.

[3] E. Richard, A. Tijou, P. Richard, and J.-L. Ferrier, "Multi-modal virtual environments for education with haptic and olfactory feedback," *Virtual Reality*, vol. 10, no. 3-4, pp. 207–225, 2006.

[4] C. S. Gulas and P. H. Bloch, "Right under our noses: ambient scent and consumer responses," *Journal of Business and Psychology*, vol. 10, no. 1, pp. 87–98, 1995.

[5] M. Lyons, S. Akamatsu, M. Kamachi, and J. Gyoba, "Coding facial expressions with gabor wavelets," in *Automatic Face and Gesture Recognition, 1998. Proceedings. Third IEEE International Conference on*. IEEE, 1998, pp. 200–205.

[6] I. E. De Araujo, E. T. Rolls, M. L. Kringelbach, F. McGlone, and N. Phillips, "Taste-olfactory convergence, and the representation of the pleasantness of flavour, in the human brain," *European Journal of Neuroscience*, vol. 18, no. 7, pp. 2059–2068, 2003.

[7] F. S. Bellezza, A. G. Greenwald, and M. R. Banaji, "Words high and low in pleasantness as rated by male and female college students," *Behavior Research Methods, Instruments, & Computers*, vol. 18, no. 3, pp. 299–303, 1986.

[8] R. J. Zatorre, M. Jones-Gotman, and C. Rouby, "Neural mechanisms involved in odor pleasantness and intensity judgments," *Neuroreport*, vol. 11, no. 12, pp. 2711–2716, 2000.

[9] M. L. Kringelbach, J. ODoherty, E. T. Rolls, and C. Andrews, "Activation of the human orbitofrontal cortex to a liquid food stimulus is correlated with its subjective pleasantness," *Cerebral Cortex*, vol. 13, no. 10, pp. 1064–1071, 2003.

[10] E. Kroupi, A. Yazdani, J.-M. Vesin, and T. Ebrahimi, "Eeg correlates of pleasant and unpleasant odor perception," *ACM Transactions on Multimedia Computing, Communications, and Applications (TOMM)*, vol. 11, no. 1s, p. 13, 2014.

[11] ——, "Multivariate spectral analysis for identifying the brain activations during olfactory perception," in *Engineering in Medicine and Biology Society (EMBC), 2012 Annual International Conference of the IEEE*. IEEE, 2012, pp. 6172–6175.

[12] P. Joussain, M. Thevenet, C. Rouby, and M. Bensafi, "Effect of aging on hedonic appreciation of pleasant and unpleasant odors," *PloS one*, vol. 8, no. 4, p. e61376, 2013.

[13] M. D. Greicius, B. H. Flores, V. Menon, G. H. Glover, H. B. Solvason, H. Kenna, A. L. Reiss, and A. F. Schatzberg, "Resting-state functional connectivity in major depression: abnormally increased contributions from subgenual cingulate cortex and thalamus," *Biological psychiatry*, vol. 62, no. 5, pp. 429–437, 2007.

[14] A. B. Waites, R. S. Briellmann, M. M. Saling, D. F. Abbott, and G. D. Jackson, "Functional connectivity networks are disrupted in left temporal lobe epilepsy," *Annals of neurology*, vol. 59, no. 2, pp. 335–343, 2006.

[15] M. P. Van Den Heuvel and H. E. Hulshoff Pol, "Exploring the brain network: a review on resting-state fmri functional connectivity," *European Neuropsychopharmacology*, vol. 20, no. 8, pp. 519–534, 2010.

[16] C. W. Granger, "Investigating causal relations by econometric models and cross-spectral methods," *Econometrica: Journal of the Econometric Society*, pp. 424–438, 1969.

[17] T. Schreiber, "Measuring information transfer," *Physical review letters*, vol. 85, no. 2, p. 461, 2000.

[18] J. Pijn, P. Vijn, F. Lopes da Silva, W. Van Ende Boas, and W. Blanes, "Localization of epileptogenic foci using a new signal analytical approach," *Neurophysiologie Clinique/Clinical Neurophysiology*, vol. 20, no. 1, pp. 1–11, 1990.

[19] F. T. Sun, L. M. Miller, and M. D'Esposito, "Measuring interregional functional connectivity using coherence and partial coherence analyses of fmri data," *Neuroimage*, vol. 21, no. 2, pp. 647–658, 2004.

[20] D. J. Watts and S. H. Strogatz, "Collective dynamics of small-worldnetworks," *nature*, vol. 393, no. 6684, pp. 440–442, 1998.

[21] V. Latora and M. Marchiori, "Efficient behavior of small-world networks," *Physical review letters*, vol. 87, no. 19, p. 198701, 2001.

[22] F. Passerini and S. Severini, "The von neumann entropy of networks," *arXiv preprint arXiv:0812.2597*, 2008.

[23] C. Wolters and J. C. de Munck, "Volume conduction," *Scholarpedia*, vol. 2, no. 3, p. 1738, 2007.

[24] S. J. Luck, *An introduction to the event-related potential technique*. MIT press, 2014.

[25] O. Sporns, "Brain connectivity," *Scholarpedia*, vol. 2, no. 10, p. 4695, 2007.

[26] G. Bettus, F. Wendling, M. Guye, L. Valton, J. Régis, P. Chauvel, and F. Bartolomei, "Enhanced eeg functional connectivity in mesial temporal lobe epilepsy," *Epilepsy research*, vol. 81, no. 1, pp. 58–68, 2008.

[27] A. Roebroeck, E. Formisano, and R. Goebel, "Mapping directed influence over the brain using granger causality and fmri," *Neuroimage*, vol. 25, no. 1, pp. 230–242, 2005.

[28] L. Barnett and A. K. Seth, "The mvgc multivariate granger causality toolbox: A new approach to granger-causal inference," *Journal of neuroscience methods*, vol. 223, pp. 50–68, 2014.

[29] M. Morf, A. Vieira, D. Lee, and T. Kailath, "Recursive multichannel maximum entropy spectral estimation," *IEEE Trans. Geosci. Electron*, vol. 16, no. 2, pp. 85–94, 1978.

[30] R. Oostenveld, P. Fries, E. Maris, and J.-M. Schoffelen, "Fieldtrip: open source software for advanced analysis of MEG, EEG, and invasive electrophysiological data," *Computational intelligence and neuroscience*, vol. 2011, 2010.

[31] V. M. Eguiluz, D. R. Chialvo, G. A. Cecchi, M. Baliki, and A. V. Apkarian, "Scale-free brain functional networks," *Physical review letters*, vol. 94, no. 1, p. 018102, 2005.

[32] D. S. Bassett and E. Bullmore, "Small-world brain networks," *The neuroscientist*, vol. 12, no. 6, pp. 512–523, 2006.

[33] J. R. Ullmann, "An algorithm for subgraph isomorphism," *Journal of the ACM (JACM)*, vol. 23, no. 1, pp. 31–42, 1976.

[34] C. J. Stam, "Functional connectivity patterns of human magnetoencephalographic recordings: a small-worldnetwork?" *Neuroscience letters*, vol. 355, no. 1, pp. 25–28, 2004.

[35] K. Anand and G. Bianconi, "Entropy measures for networks: Toward an information theory of complex topologies," *Physical Review E*, vol. 80, no. 4, p. 045102, 2009.

[36] J. S. Uebersax, "Diversity of decision-making models and the measurement of interrater agreement." *Psychological Bulletin*, vol. 101, no. 1, p. 140, 1987.